An improved stochastic algorithm for temperature-dependent homogeneous gas phase reactions

Markus Kraft [*], Wolfgang Wagner

Department of Chemical Engineering, University of Cambridge, Pembroke Street, Cambridge CB2 3RA, UK
Weierstrass Institute for Applied Analysis and Stochastics, Berlin, Germany

Abstract

We propose an improved stochastic algorithm for temperature-dependent homogeneous gas phase reactions. By combining forward and reverse reaction rates, a significant gain in computational efficiency is achieved. Two modifications of modelling the temperature dependence (with and without conservation of enthalpy) are introduced and studied quantitatively. The algorithm is tested for the combustion of *n*-heptane, which is a reference fuel component for internal combustion engines. The convergence of the algorithm is studied by a series of numerical experiments and the computational cost of the stochastic algorithm is compared with the DAE code DASSL. If less accuracy is needed the stochastic algorithm is faster on short simulation time intervals. The new stochastic algorithm is significantly faster than the original direct simulation algorithm in all cases considered.
© 2002 Elsevier Science B.V. All rights reserved.

Keywords: Homogeneous gas phase reaction; Stochastic algorithm; Markov process; Temperature algorithm; Partial equilibrium

1. Introduction

In this paper we present an improved stochastic algorithm that computes the time evolution of a homogeneous reacting gas mixture in a closed adiabatic system with constant pressure. The *reaction mechanism* consists of several elementary chemical reactions

$$(v_{\alpha,1}, \ldots, v_{\alpha,S}) \leftrightarrow (v^*_{\alpha,1}, \ldots, v^*_{\alpha,S}), \quad \alpha = 1, \ldots, I, \tag{1.1}$$

where S is the number of chemical species and I is the number of possible reactions. The stoichiometric coefficients $v_{\alpha,i}$ and $v^*_{\alpha,i}$ of the species i in reaction α are non-negative integer values.

The time evolution of the *state variables* is given by the following initial value problem (cf. [12], [15, formula (2); Ch. II, formulas (49), (52), (58)])

[*] Corresponding author. Tel.: +44-1223-762784; fax: +44-1223-334796.
E-mail addresses: markus_kraft@cheng.cam.ac.uk (M. Kraft), wagner@wias-berlin.de (W. Wagner).

$$\frac{\mathrm{d}Y_i}{\mathrm{d}t} = \frac{W_i}{\varrho}\dot{\omega}_i, \qquad Y_i(0) = Y_{0,i}, \quad i = 1,\ldots,S, \tag{1.2}$$

with the chemical production rate of the ith species

$$\dot{\omega}_i = \sum_{\alpha=1}^{I}(v_{\alpha,i}^* - v_{\alpha,i})q_\alpha \tag{1.3}$$

and the rate of progress of the αth reaction

$$q_\alpha = [M_\alpha]\left(K_{\alpha,f}\prod_{k=1}^{S}[X_k]^{v_{\alpha,k}} - K_{\alpha,r}\prod_{k=1}^{S}[X_k]^{v_{\alpha,k}^*}\right). \tag{1.4}$$

Here Y, $[X]$ and W denote the vectors of the mass fractions, the molar concentrations, and the molecular weights of the species, respectively. The mass density is denoted by ϱ. The numbers $K_{\alpha,f}$ and $K_{\alpha,r}$ are the forward and reverse rate constants for the αth reaction, which are assumed to have the following Arrhenius temperature dependence

$$K_{\alpha,f} = A_{\alpha,f}T^{\beta_{\alpha,f}}\exp(-E_{\alpha,f}/RT), \tag{1.5}$$

$$K_{\alpha,r} = A_{\alpha,r}T^{\beta_{\alpha,r}}\exp(-E_{\alpha,r}/RT),$$

where $A_{\alpha,f}, A_{\alpha,r}$ are pre-exponential factors, $\beta_{\alpha,f}, \beta_{\alpha,r}$ are temperature exponents and $E_{\alpha,f}, E_{\alpha,r}$ are activation energies. The factor $[M_\alpha] = \sum_{k=1}^{S}B_{\alpha,k}[X_k]$ takes into account that, in some reactions, a "third body" is required for the reaction to proceed. If no third body is needed, then $[M_\alpha] = 1$. The time evolution of the *temperature* is given by the equation (cf. [15, formula (15)])

$$\frac{\mathrm{d}T}{\mathrm{d}t} = -\frac{1}{c_p\varrho}\sum_{k=1}^{S}h_k W_k\dot{\omega}_k = -\frac{1}{c_p}\sum_{k=1}^{S}h_k\frac{\mathrm{d}Y_k}{\mathrm{d}t}, \tag{1.6}$$

where h is the vector of specific enthalpies, and c_p is the mean specific heat capacity.

One of the first publications on calculating homogeneous reaction systems using stochastic ideas is Bunker et al. [4]. In that paper an algorithm was proposed to simulate the combustion of propane in an adiabatic plug flow reactor. Independently, Gillespie suggested an algorithm that mimics the dynamics of any well stirred gas mixture of reactive chemical species in thermal equilibrium [9]. In that algorithm it is assumed that temperature is constant. This approach can be viewed as a mesoscopic description of chemical reactions that is between the macroscopic description, given by particle densities averaged over a control volume, and the microscopic description given by the momentum and the position of all molecules contained in the control volume. By studying a steady state solution of the Lotka reaction system, Gillespie demonstrated that the stochastic algorithm is able to account for microscopic fluctuations [10]. Very recently this direct simulation algorithm has been used to study chaos in chemical systems [17].

Stochastic algorithms based on [4,9] have been applied by several authors for various purposes. For example in [2] the formation of soot using a coagulation reaction model has been investigated. Also reaction diffusion problems have been studied using the algorithm in conjunction with components that account for the diffusion process. The Fisher equation was studied in [3], and the Maginu equation was investigated in [6]. Another area where the algorithm has been extensively applied is the modelling of surface processes [8]. For example the temperature-programmed desorption was studied in [11,16]. In [13] a detailed numerical study of the convergence properties of the Gillespie algorithm was performed.

The *purpose of this paper* is to introduce an improved stochastic algorithm, to present two alternative methods to include temperature dependence, and to study its convergence and performance properties. In contrast to the direct simulation approach by Bunker et al. and Gillespie, the new algorithm is based on combining forward and reverse reactions in order to achieve better efficiency, when partial equilibria are reached. The algorithm contains various mechanisms of approximating the temperature step during an elementary reaction – a simple first order approach, and an iteration scheme preserving enthalpy. The algorithm is applied to a real combustion problem using a practically relevant fuel.

The paper is organized as follows. Section 2 is concerned with the description of the stochastic model. The basic Markov jump process is defined, and relevant combustion quantities are represented in terms of related random variables. The deterministic Eqs. (1.2), (1.3), (1.4), and (1.6) are derived from the stochastic system. Finally, the corresponding stochastic algorithm is described. Results of numerical experiments are presented in Section 3. The algorithm is applied to simulate the ignition of heptane. Heptane chemistry is modelled with a detailed chemical mechanism that includes 107 species and 808 reversible reactions. It is compared with an accurate deterministic method based on the solver DASSL for systems of stiff ordinary differential equations. The first part of test calculations is concerned with the convergence behaviour of the algorithm. In the second part the issue of performance is studied, and limitations of the present algorithm are illustrated. Finally some conclusions are drawn in Section 4.

2. The stochastic model

2.1. Markov process

In this section we provide a detailed description of the stochastic algorithm. First we introduce the corresponding Markov process in an abstract setting. Then we show how relevant combustion quantities are represented in terms of this process. Special attention is paid to various approximations of the temperature step. Next the deterministic equations are derived in the limit of an increasing particle number. Finally, the algorithm is described as a method of averaging of functionals on trajectories of the Markov process.

We consider a Markov process of the form

$$Z^{(n)}(t) = \left(N_1^{(n)}(t), \dots, N_S^{(n)}(t), T^{(n)}(t) \right), \quad t \geqslant 0, \tag{2.1}$$

where $N_j^{(n)}(t) \in \{0, 1, \dots\}$ denotes the number of particles of type $j = 1, \dots, S$ and $T^{(n)}(t) > 0$ denotes temperature at time t. The number of particles at time zero

$$n = \sum_{j=1}^{S} N_j^{(n)}(0)$$

plays the role of an approximation parameter. Concerning the *initial state*, it is assumed that

$$\lim_{n \to \infty} \frac{N_i^{(n)}(0)}{n} = \lambda_i^0, \quad i = 1, \dots, S, \tag{2.2}$$

and

$$T^{(n)}(0) = T^0 \tag{2.3}$$

for some constants λ_i^0, T^0.

The stochastic system (2.1) is a pure jump process defined by the *generator*

$$(\mathscr{A}\Phi)(x) = \sum_{\alpha=1}^{I} Q_\alpha(x)[\Phi(J_\alpha(x)) - \Phi(x)], \quad x \in \{0, 1, \ldots\}^S \times \mathscr{R}_+, \tag{2.4}$$

where Φ is some test function. The distribution of the random jumps is determined by *rate functions* of the form

$$Q_\alpha(x) = |Q_{\alpha,f}(x) - Q_{\alpha,r}(x)|, \tag{2.5}$$

where (cf. (1.1) and (1.5))

$$Q_{\alpha,f}(x) = \gamma(x)^{1-\sum_{j=1}^{S} v_{\alpha,j}} M_\alpha(x) K_{\alpha,f}(x_{S+1}) \prod_{j=1}^{S} \prod_{i=0}^{v_{\alpha,j}-1} (x_j - i), \tag{2.6}$$

$$Q_{\alpha,r}(x) = \gamma(x)^{1-\sum_{j=1}^{S} v_{\alpha,j}^*} M_\alpha(x) K_{\alpha,r}(x_{S+1}) \prod_{j=1}^{S} \prod_{i=0}^{v_{\alpha,j}^*-1} (x_j - i), \tag{2.7}$$

and

$$M_\alpha(x) = \begin{cases} \sum_{k=1}^{S} B_{\alpha,k} \frac{x_k}{\gamma(x)} & \text{if third body reaction with some species,} \\ \frac{p}{R x_{S+1}} & \text{if third body reaction with all species,} \\ 1 & \text{otherwise.} \end{cases} \tag{2.8}$$

The function γ is a normalization parameter. The choice

$$\gamma(x) = \frac{R x_{S+1}}{p} \sum_{j=1}^{S} x_j \tag{2.9}$$

corresponds to normalization with volume (cf. (2.17) below). The process performs jumps according to the *jump transformation*

$$J_\alpha(x) = \begin{cases} J_{\alpha,f}(x) & \text{if} \quad Q_{\alpha,f}(x) \geqslant Q_{\alpha,r}(x), \\ J_{\alpha,r}(x) & \text{otherwise,} \end{cases} \tag{2.10}$$

where

$$J_{\alpha,f}(x) = (x_1 - v_{\alpha,1} + v_{\alpha,1}^*, \ldots, x_S - v_{\alpha,S} + v_{\alpha,S}^*, x_{S+1} + \Delta T_{\alpha,f}(x)) \tag{2.11}$$

and

$$J_{\alpha,r}(x) = (x_1 - v_{\alpha,1}^* + v_{\alpha,1}, \ldots, x_S - v_{\alpha,S}^* + v_{\alpha,S}, x_{S+1} + \Delta T_{\alpha,r}(x)). \tag{2.12}$$

Remark. The second products in (2.6) and (2.7) assure that a reaction may only occur if there are enough of the corresponding particles in the system (cf. (2.11) and (2.12)). Note that these products are zero if $x_j < v_{\alpha,j}$ (or $x_j < v_{\alpha,j}^*$, respectively) for some $j = 1, \ldots, S$. They are defined to be 1 in the case $v_{\alpha,j} = 0$ or $v_{\alpha,j}^* = 0$, respectively.

By definition, *mass conservation* means (cf. (2.10)–(2.12))

$$\sum_{j=1}^{S} W_j J_\alpha(x)_j = \sum_{j=1}^{S} W_j x_j. \tag{2.13}$$

This property holds provided that

$$\sum_{i=1}^{S} W_i v_{\alpha,i} = \sum_{i=1}^{S} W_i v_{\alpha,i}^*, \quad \alpha = 1, \ldots, I. \tag{2.14}$$

The basic theoretical result concerning the Markov process (2.1) is that, under assumptions (2.2) and (2.3)

$$\lim_{n \to \infty} \frac{N_i^{(n)}(t)}{n} = \lambda_i(t), \quad i = 1, \ldots, S, \quad t > 0, \tag{2.15}$$

and

$$\lim_{n \to \infty} T^{(n)}(t) = T(t), \quad t > 0. \tag{2.16}$$

Later we will formally derive equations, which are satisfied by the limit of the stochastic process. For a rigorous approach we refer to [7, p. 454]. These limiting equations can be numerically solved by the corresponding stochastic algorithm.

2.2. Physical quantities

Here we discuss how relevant physical quantities are represented in terms of the random variables $N_k^{(n)}(t)$, $k = 1, \ldots, S$ (cf. (2.1)), which correspond to the mole numbers $n_k(t)$ in the chemical literature.

The *total mole number* is

$$n(t) = \sum_{k=1}^{S} n_k(t) \sim \sum_{k=1}^{S} N_k^{(n)}(t),$$

the *total mass* is

$$m(t) = \sum_{k=1}^{S} W_k n_k(t) \sim \sum_{k=1}^{S} W_k N_k^{(n)}(t),$$

and the *volume* is

$$V(t) = \frac{RT(t)}{p} n(t) \sim \frac{RT^{(n)}(t)}{p} \sum_{k=1}^{S} N_k^{(n)}(t), \tag{2.17}$$

where W denotes the vector of the molecular weights of the species, T and p denote temperature and pressure, respectively, and R is a gas constant. Note that

$$\frac{1}{n} \sum_{k=1}^{S} N_k^{(n)}(t) \xrightarrow{n} \sum_{k=1}^{S} \lambda_k(t) =: \tilde{\boldsymbol{n}}(t),$$

$$\frac{1}{n} \sum_{k=1}^{S} W_k N_k^{(n)}(t) \xrightarrow{n} \sum_{k=1}^{S} W_k \lambda_k(t) =: \tilde{\boldsymbol{m}}(t), \tag{2.18}$$

and

$$\frac{1}{n} \frac{RT^{(n)}(t)}{p} \sum_{j} N_j^{(n)}(t) \xrightarrow{n} \frac{RT(t)}{p} \sum_{k=1}^{S} \lambda_k(t) =: \tilde{V}(t) = \frac{RT(t)}{p} \tilde{\boldsymbol{n}}(t). \tag{2.19}$$

Remark. The quantities $n(t)$, $m(t)$, $V(t)$ are of physical size (large values). They are obtained from the quantities $\tilde{n}(t), \tilde{m}(t), \tilde{V}(t)$ (which are calculated using the limit functions $\lambda_i(t)$) by multiplication with the appropriate initial total mole number $n(0)$. The quantities below are normalized (moderate values), and we will use the same symbols for both the physical quantities and the quantities obtained using $\lambda_i(t)$.

The *mole fraction* of a species k is given by

$$X_k(t) = \frac{n_k(t)}{n(t)} \sim \frac{N_k^{(n)}(t)}{\sum_j N_j^{(n)}(t)} \xrightarrow{n} \frac{\lambda_k(t)}{\sum_j \lambda_j(t)} = \frac{\lambda_k(t)}{\tilde{\boldsymbol{n}}(t)},$$

its *mass fraction* is

$$Y_k(t) = \frac{W_k n_k(t)}{m(t)} \sim \frac{W_k N_k^{(n)}(t)}{\sum_j W_j N_j^{(n)}(t)} \xrightarrow{n} \frac{W_k \lambda_k(t)}{\sum_j W_j \lambda_j(t)} = \frac{W_k \lambda_k(t)}{\tilde{\boldsymbol{m}}(t)}, \tag{2.20}$$

and the *molar concentration* is

$$[X_k](t) = \frac{n_k(t)}{V(t)} \sim \frac{N_k^{(n)}(t)}{(RT^{(n)}(t)/p) \sum_j N_j^{(n)}(t)} \xrightarrow{n} \frac{\lambda_k(t)}{(RT(t)/p) \sum_j \lambda_j(t)} = \frac{\lambda_k(t)}{\tilde{V}(t)}. \tag{2.21}$$

The *mass density* is

$$\varrho(t) = \frac{m(t)}{V(t)} = \frac{\sum_{k=1}^{S} W_k n_k(t)}{V(t)} = \sum_{k=1}^{S} W_k [X_k](t) \sim \frac{\sum_k W_k N_k^{(n)}(t)}{(RT/p) \sum_j N_j^{(n)}(t)} \xrightarrow{n} \frac{\tilde{\boldsymbol{m}}(t)}{\tilde{V}(t)}. \tag{2.22}$$

One obtains from the definitions that

$$\sum_{k=1}^{S} Y_k(t) = 1, \quad \sum_{k=1}^{S} X_k(t) = 1, \quad \sum_{k=1}^{S} [X_k](t) = \frac{n(t)}{V(t)} = \frac{p}{RT(t)},$$

and

$$\frac{Y_k(t)}{W_k} = \frac{X_k(t)}{\overline{W}(t)} = \frac{[X_k](t)}{\varrho(t)},$$

where

$$\overline{W}(t) = \sum_{k=1}^{S} W_k X_k(t) = \frac{1}{n(t)} \sum_{k=1}^{S} W_k n_k(t) = \frac{m(t)}{n(t)}$$

is the *mean molecular weight*.

Further quantities, relevant for temperature considerations, are *enthalpy* $H_k(T)$, *specific enthalpy* $h_k(T) = H_k(T)/W_k$, *heat capacity* $C_k(T)$ and *specific heat capacity* (at constant pressure) $c_k(T) = C_k(T)/W_k$. Note that [15, Ch. II, formula (15)]

$$c_k(T) = \frac{\mathrm{d}}{\mathrm{d}T} h_k(T). \tag{2.23}$$

The *mean enthalpy* is

$$H(t) = \sum_{k=1}^{S} H_k(T(t)) X_k(t) \sim \frac{\sum_{k=1}^{S} H_k(T^{(n)}(t)) N_k^{(n)}(t)}{\sum_j N_j^{(n)}(t)} \xrightarrow{n} \frac{\sum_k H_k(T(t)) \lambda_k(t)}{\sum_j \lambda_j(t)},$$

the *mean specific enthalpy* is

$$h(t) = \sum_{k=1}^{S} h_k(T(t))Y_k(t) \sim \frac{\sum_{k=1}^{S} H_k(T^{(n)}(t))N_k^{(n)}(t)}{\sum_j W_j N_j^{(n)}(t)} \xrightarrow{n} \frac{\sum_k H_k(T(t))\lambda_k(t)}{\sum_j W_j \lambda_j(t)}, \tag{2.24}$$

the *mean heat capacity* is

$$C(t) = \sum_{k=1}^{S} C_k(T(t))X_k(t) \sim \frac{\sum_{k=1}^{S} C_k(T^{(n)}(t))N_k^{(n)}(t)}{\sum_j N_j^{(n)}(t)} \xrightarrow{n} \frac{\sum_k C_k(T(t))\lambda_k(t)}{\sum_j \lambda_j(t)}, \tag{2.25}$$

and the *mean specific heat capacity* is

$$c(t) = \sum_{k=1}^{S} c_k(T(t))Y_k(t) \sim \frac{\sum_{k=1}^{S} C_k(T^{(n)}(t))N_k^{(n)}(t)}{\sum_j W_j N_j^{(n)}(t)} \xrightarrow{n} \frac{\sum_k C_k(T(t))\lambda_k(t)}{\sum_j W_j \lambda_j(t)}. \tag{2.26}$$

Note that from definitions (2.24) and (2.23) one obtains

$$\frac{d}{dt}h(t) = \sum_k h_k(T(t))\frac{d}{dt}Y_k(t) + \sum_k Y_k(t)c_k(T(t))\frac{d}{dt}T(t).$$

Thus, the *enthalpy conservation* property [15, formula (13)]

$$\frac{d}{dt}h(t) = 0 \tag{2.27}$$

and the definition (2.26) imply (cf. (1.6))

$$\frac{d}{dt}T(t) = -\frac{1}{c(t)} \sum_{k=1}^{S} h_k(T(t))\frac{d}{dt}Y_k(t). \tag{2.28}$$

2.3. Temperature step

Here we construct concrete expressions for the terms $\Delta T_{\alpha,f}(x), \Delta T_{\alpha,r}(x)$ in (2.11) and (2.12). Using (2.26) and (2.20), Eq. (2.28) may be rewritten as

$$\frac{d}{dt}T(t) = -\frac{\sum_k H_k(T(t))(d/dt)n_k(t)}{\sum_k C_k(T(t))n_k(t)}. \tag{2.29}$$

Note that

$$N_k^{(n)}(t + \Delta t) - N_k^{(n)}(t) = v_{\alpha,k}^* - v_{\alpha,k}, \tag{2.30}$$

in case (2.11), and

$$N_k^{(n)}(t + \Delta t) - N_k^{(n)}(t) = v_{\alpha,k} - v_{\alpha,k}^*, \tag{2.31}$$

in case (2.12). These relations and (2.29) suggest *first order approximations* of the form

$$\Delta T_{\alpha,f}(x) = -\frac{\sum_{k=1}^{S} H_k(x_{S+1})[v_{\alpha,k}^* - v_{\alpha,k}]}{\sum_{k=1}^{S} C_k(x_{S+1})x_k}, \tag{2.32}$$

$$\Delta T_{\alpha,r}(x) = -\frac{\sum_{k=1}^{S} H_k(x_{S+1})[v_{\alpha,k} - v_{\alpha,k}^*]}{\sum_{k=1}^{S} C_k(x_{S+1})x_k}. \tag{2.33}$$

Next we construct a temperature step taking into account the conservation property (2.27). One observes that mass conservation (2.14) implies (cf. 2.30 and 2.31)

$$\sum_{k=1}^{S} W_k N_k^{(n)}(t + \Delta t) = \sum_{k=1}^{S} W_k N_k^{(n)}(t).$$

Thus, (2.27) and (2.24) suggest an *enthalpy preserving approximation* of the temperature step $T^{(n)}(t + \Delta t) - T^{(n)}(t)$ defined via the equation

$$\sum_{k=1}^{S} H_k(T^{(n)}(t + \Delta t))N_k^{(n)}(t + \Delta t) = \sum_{k=1}^{S} H_k(T^{(n)}(t))N_k^{(n)}(t). \tag{2.34}$$

In order to solve (2.34) with respect to $T^{(n)}(t + \Delta t)$ we introduce the function

$$f(x) := \sum_k H_k(x)N_k^{(n)}(t + \Delta t) - \sum_k H_k(T^{(n)}(t))N_k^{(n)}(t),$$

an iteration scheme

$$T_{i+1} := T_i - \frac{f(T_i)}{f'(T_i)}, \quad T_0 := T^{(n)}(t),$$

and define

$$T^{(n)}(t + \Delta t) = \lim_{i \to \infty} T_i.$$

From (2.23) one obtains

$$f'(x) = \sum_k C_k(x)N_k^{(n)}(t + \Delta t)$$

so that

$$T_{i+1} = T_i - \frac{\sum_k H_k(T_i)N_k^{(n)}(t + \Delta t) - \sum_k H_k(T_0)N_k^{(n)}(t)}{\sum_k C_k(T_i)N_k^{(n)}(t + \Delta t)}. \tag{2.35}$$

2.4. Asymptotic behaviour

The Markov process (2.1) satisfies

$$\Phi(Z^{(n)}(t)) = \Phi(Z^{(n)}(0)) + \int_0^t (\mathscr{A}\Phi)(Z^{(n)}(s)) \, ds + \mu^{(n)}(t), \quad t \geqslant 0, \tag{2.36}$$

where $\mu^{(n)}(t)$ is a martingale term vanishing in the limit $n \to \infty$. The representation (2.36) suggests that (cf. (2.4))

$$\frac{d}{dt} \lim_{n \to \infty} \Phi(Z^{(n)}(t)) = \sum_{\alpha=1}^{I} \lim_{n \to \infty} Q_\alpha(Z^{(n)}(t)) \big[\Phi(J_\alpha(Z^{(n)}(t))) - \Phi(Z^{(n)}(t))\big]. \tag{2.37}$$

Since (cf. (2.6))

$$Q_{\alpha,f}(x) = \left(\frac{\gamma(x)}{n}\right)^{1-\sum_{j=1}^{S} v_{\alpha,j}} n M_\alpha(x) K_{\alpha,f}(x_{S+1}) \prod_{j=1}^{S} \frac{x_j(x_j - 1) \cdots (x_j + 1 - v_{\alpha,j})}{n^{v_{\alpha,j}}},$$

and, according to (2.15) and (2.16),

$$\lim_{n \to \infty} \frac{N_j^{(n)}(t)(N_j^{(n)}(t) - 1) \cdots (N_j^{(n)}(t) + 1 - v_{\alpha,j})}{n^{v_{\alpha,j}}} = \lambda_j(t)^{v_{\alpha,j}},$$

one obtains

$$\lim_{n \to \infty} \frac{1}{n} Q_{\alpha,f}(Z^{(n)}(t)) = \tilde{\gamma}(t) \tilde{M}_\alpha(t) K_{\alpha,f}(T(t)) \prod_{j=1}^{S} \left[\frac{\lambda_j(t)}{\tilde{\gamma}(t)}\right]^{v_{\alpha,j}} \tag{2.38}$$

and, analogously (cf. (2.7)),

$$\lim_{n \to \infty} \frac{1}{n} Q_{\alpha,r}(Z^{(n)}(t)) = \tilde{\gamma}(t) \tilde{M}_\alpha(t) K_{\alpha,r}(T(t)) \prod_{j=1}^{S} \left[\frac{\lambda_j(t)}{\tilde{\gamma}(t)}\right]^{v_{\alpha,j}^*}, \tag{2.39}$$

where the notations

$$\tilde{\gamma}(t) = \lim_{n \to \infty} \frac{1}{n} \gamma(Z^{(n)}(t)) \tag{2.40}$$

and

$$\tilde{M}_\alpha(t) = \lim_{n \to \infty} M_\alpha(Z^{(n)}(t))$$

have been used. Note that (cf. (2.8), (2.15), and (2.16))

$$\tilde{M}_\alpha(t) = \begin{cases} \sum_{k=1}^{S} B_{\alpha,k} \frac{\lambda_k(t)}{\tilde{\gamma}(t)} & \text{if third body reaction with some species,} \\ \frac{p}{RT(t)} & \text{if third body reaction with all species,} \\ 1 & \text{otherwise.} \end{cases} \tag{2.41}$$

Thus, Eq. (2.37) takes the form (cf. (2.5))

$$\frac{\mathrm{d}}{\mathrm{d}t} \lim_{n \to \infty} \Phi(Z^{(n)}(t)) = \tilde{\gamma}(t) \sum_{\alpha=1}^{I} \tilde{M}_\alpha(t) \left| K_{\alpha,f}(T(t)) \prod_{j=1}^{S} \left[\frac{\lambda_j(t)}{\tilde{\gamma}(t)}\right]^{v_{\alpha,j}} \right.$$

$$\left. - K_{\alpha,r}(T(t)) \prod_{j=1}^{S} \left[\frac{\lambda_j(t)}{\tilde{\gamma}(t)}\right]^{v_{\alpha,j}^*} \right| \lim_{n \to \infty} n \left[\Phi(J_\alpha(Z^{(n)}(t))) - \Phi(Z^{(n)}(t))\right]. \tag{2.42}$$

First we derive the *equations for the state variables* (1.2)–(1.4). Consider the test functions

$$\Phi_i(x) = \frac{W_i x_i}{\sum_{j=1}^{S} W_j x_j}, \quad i = 1, \ldots, S,$$

and note that (cf. (2.20))

$$\lim_{n \to \infty} \Phi_i(Z^{(n)}(t)) = \frac{W_i \lambda_i(t)}{\sum_{j=1}^{S} W_j \lambda_j(t)} = Y_i(t).$$

According to (2.13) one obtains

$$\Phi_i(J_{\alpha,f}(x)) - \Phi_i(x) = \frac{1}{\sum_{j=1}^{S} W_j x_j} \left[W_i(x_i - v_{\alpha,i} + v_{\alpha,i}^*) - W_i x_i \right] = \frac{1}{\sum_{j=1}^{S} W_j x_j} \left[W_i(v_{\alpha,i}^* - v_{\alpha,i}) \right]$$

so that (cf. (2.18))

$$\lim_{n \to \infty} n \left[\Phi_i(J_{\alpha,f}(Z^{(n)}(t))) - \Phi_i(Z^{(n)}(t)) \right] = \frac{1}{\tilde{m}(t)} \left[W_i(v_{\alpha,i}^* - v_{\alpha,i}) \right]$$

and, analogously,

$$\lim_{n \to \infty} n \left[\Phi_i(J_{\alpha,r}(Z^{(n)}(t))) - \Phi_i(Z^{(n)}(t)) \right] = \frac{1}{\tilde{m}(t)} \left[W_i(v_{\alpha,i} - v_{\alpha,i}^*) \right].$$

Using (2.10), we obtain

$$\lim_{n \to \infty} n \left[\Phi_i(J_\alpha(Z^{(n)}(t))) - \Phi_i(Z^{(n)}(t)) \right]$$

$$= \begin{cases} \frac{1}{\tilde{m}(t)} \left[W_i(v_{\alpha,i}^* - v_{\alpha,i}) \right] & \text{if } \lim_{n \to \infty} \frac{1}{n} Q_{\alpha,f}(Z^{(n)}(t)) \geqslant \lim_{n \to \infty} \frac{1}{n} Q_{\alpha,r}(Z^{(n)}(t)), \\ \frac{1}{\tilde{m}(t)} \left[W_i(v_{\alpha,i} - v_{\alpha,i}^*) \right] & \text{otherwise.} \end{cases}$$

Thus, Eq. (2.42) implies (cf. (2.38) and (2.39))

$$\frac{\mathrm{d}}{\mathrm{d}t} Y_i(t) = \frac{\tilde{\gamma}(t)}{\tilde{m}(t)} \sum_{\alpha=1}^{I} \tilde{M}_\alpha(t) \left[K_{\alpha,f}(T(t)) \prod_{j=1}^{S} \left[\frac{\lambda_j(t)}{\tilde{\gamma}(t)} \right]^{v_{\alpha,j}} - K_{\alpha,r}(T(t)) \prod_{j=1}^{S} \left[\frac{\lambda_j(t)}{\tilde{\gamma}(t)} \right]^{v_{\alpha,j}^*} \right] \left[W_i(v_{\alpha,i}^* - v_{\alpha,i}) \right]. \quad (2.43)$$

With the choice (2.9) one obtains (cf. (2.19) and (2.40))

$$\tilde{\gamma}(t) = \tilde{V}(t) \quad (2.44)$$

and Eq. (2.43) takes the form (cf. (2.21) and (2.22))

$$\frac{\mathrm{d}}{\mathrm{d}t} Y_i(t) = \frac{W_i}{\varrho(t)} \sum_{\alpha=1}^{I} [v_{\alpha,i}^* - v_{\alpha,i}] \tilde{M}_\alpha(t) \left(K_{\alpha,f}(T(t)) \prod_{j=1}^{S} [X_j](t)^{v_{\alpha,j}} - K_{\alpha,r}(T(t)) \prod_{j=1}^{S} [X_j](t)^{v_{\alpha,j}^*} \right), \quad (2.45)$$

where (cf. (2.41))

$$\tilde{M}_\alpha(t) = \begin{cases} \sum_{k=1}^{S} B_{\alpha,k} [X_k](t) & \text{if third body reaction with some species,} \\ \frac{p}{RT(t)} & \text{if third body reaction with all species,} \\ 1 & \text{otherwise.} \end{cases}$$

Note that, up to notations, Eq. (2.45) is identical with (1.2), (1.3), (1.4).

Next we derive the *equation for the temperature* (1.6). Consider the test function

$$\Phi(x) = x_{S+1}$$

and note that (cf. (2.1) and (2.16))

$$\lim_{n \to \infty} \Phi(Z^{(n)}(t)) = T(t). \quad (2.46)$$

According to (2.11) and (2.12) one obtains

$$\Phi(J_{\alpha,f}(x)) - \Phi(x) = \Delta T_{\alpha,f}(x)$$

so that

$$\lim_{n\to\infty} n\left[\Phi(J_{\alpha,f}(Z^{(n)}(t))) - \Phi(Z^{(n)}(t))\right] = \lim_{n\to\infty} n\Delta T_{\alpha,f}(Z^{(n)}(t))$$

and analogously,

$$\lim_{n\to\infty} n\left[\Phi(J_{\alpha,r}(Z^{(n)}(t))) - \Phi(Z^{(n)}(t))\right] = \lim_{n\to\infty} n\Delta T_{\alpha,r}(Z^{(n)}(t)).$$

Using (2.10), we obtain

$$\lim_{n\to\infty} n\left[\Phi(J_\alpha(Z^{(n)}(t))) - \Phi(Z^{(n)}(t))\right]$$
$$= \begin{cases} \lim_{n\to\infty} n\Delta T_{\alpha,f}(Z^{(n)}(t)) & \text{if } \lim_{n\to\infty} \frac{1}{n}Q_{\alpha,f}(Z^{(n)}(t)) \geqslant \lim_{n\to\infty} \frac{1}{n}Q_{\alpha,r}(Z^{(n)}(t)), \\ \lim_{n\to\infty} n\Delta T_{\alpha,r}(Z^{(n)}(t)) & \text{otherwise.} \end{cases} \tag{2.47}$$

Assume

$$\Delta T_{\alpha,f}(x) = -\Delta T_{\alpha,r}(x) \tag{2.48}$$

so that

$$\lim_{n\to\infty} n\Delta T_{\alpha,f}(Z^{(n)}(t)) = -\lim_{n\to\infty} n\Delta T_{\alpha,r}(Z^{(n)}(t)).$$

Then, using (2.46) and (2.47), Eq. (2.42) implies

$$\frac{\mathrm{d}}{\mathrm{d}t}T(t) = \tilde{\gamma}(t)\sum_{\alpha=1}^{I}\tilde{M}_\alpha(t)\left[K_{\alpha,f}(T(t))\prod_{j=1}^{S}\left[\frac{\lambda_j(t)}{\tilde{\gamma}(t)}\right]^{v_{\alpha,j}}\right.$$
$$\left. - K_{\alpha,r}(T(t))\prod_{j=1}^{S}\left[\frac{\lambda_j(t)}{\tilde{\gamma}(t)}\right]^{v_{\alpha,j}^*}\right]\lim_{n\to\infty} n\Delta T_{\alpha,f}(Z^{(n)}(t)). \tag{2.49}$$

With the approximations (2.32) and (2.33), which fulfil (2.48), we obtain (cf. (2.15))

$$\lim_{n\to\infty} n\Delta T_{\alpha,f}(Z^{(n)}(t)) = -\frac{\sum_{k=1}^{S}H_k(T(t))[v_{\alpha,k}^* - v_{\alpha,k}]}{\sum_{k=1}^{S}C_k(T(t))\lambda_k(t)},$$

and Eq. (2.49) takes the form

$$\frac{\mathrm{d}}{\mathrm{d}t}T(t) = -\tilde{\gamma}(t)\sum_{\alpha=1}^{I}\tilde{M}_\alpha(t)\left[K_{\alpha,f}(T(t))\prod_{j=1}^{S}\left[\frac{\lambda_j(t)}{\tilde{\gamma}(t)}\right]^{v_{\alpha,j}}\right.$$
$$\left. - K_{\alpha,r}(T(t))\prod_{j=1}^{S}\left[\frac{\lambda_j(t)}{\tilde{\gamma}(t)}\right]^{v_{\alpha,j}^*}\right]\frac{\sum_{k=1}^{S}H_k(T(t))[v_{\alpha,k}^* - v_{\alpha,k}]}{\sum_{k=1}^{S}C_k(T(t))\lambda_k(t)}.$$

With the choice (2.9), this equation transforms into (cf. (2.26), (2.18), (2.22), (2.21), and (2.44))

$$\frac{\mathrm{d}}{\mathrm{d}t}T(t) = -\frac{1}{c(t)\varrho(t)}\sum_{k=1}^{S}W_k h_k(T(t))\sum_{\alpha=1}^{I}\tilde{M}_\alpha(t)[v_{\alpha,k}^* - v_{\alpha,k}]\left[K_{\alpha,f}(T(t))\prod_{j=1}^{S}[X_j](t)^{v_{\alpha,j}} - K_{\alpha,r}(T(t))\prod_{j=1}^{S}[X_j](t)^{v_{\alpha,j}^*}\right].$$

(2.50)

Taking into account (2.45), we observe that, up to notations, Eq. (2.50) is identical with (1.6).

2.5. Description of the algorithm

The stochastic algorithm for the numerical treatment of Eqs. (1.2), (1.3), (1.4), and (1.6) consists in generating trajectories of the Markov process (2.1) and averaging the appropriate functionals.

Given the state

$$x = \left(N_1^{(n)}(t), \ldots, N_S^{(n)}(t), T^{(n)}(t)\right), \quad t \geqslant 0,$$

the process remains there for a random time τ having exponential distribution with the *waiting time parameter* (cf. (2.6), (2.7), and (2.9))

$$\pi(x) = \sum_{\alpha=1}^{I}|Q_{\alpha,f}(x) - Q_{\alpha,r}(x)|,$$

(2.51)

i.e.,

$$\mathrm{Prob}(\tau \geqslant s) = \exp(-s\pi(x)), \quad s \geqslant 0.$$

At the moment $t + \tau$, a particular reaction is chosen according to the *reaction probabilities*

$$P_\alpha(x) = \frac{|Q_{\alpha,f}(x) - Q_{\alpha,r}(x)|}{\pi(x)}, \quad \alpha = 1, \ldots, I.$$

(2.52)

Finally, the process jumps into the state $J_\alpha(x)$ (cf. (2.10)), and the same procedure is repeated.

3. Numerical experiments

3.1. Test case

The test case for our study is the combustion of *n*-heptane. This example is of practical relevance, since *n*-heptane is part of the reference fuel for internal combustion engines such as spark-ignition, diesel, and gas turbine engines. The chemistry is described by a reaction mechanism containing 107 chemical species and 808 reversible reactions [5]. The initial conditions are

$$X_{n\text{-}C_7H_{16}}(0) = 0.0187, \quad X_{O_2}(0) = 0.2061, \quad X_{N_2}(0) = 0.7752.$$

Temperature and pressure are set to $T = 1500\,\mathrm{K}$ and $p = 1.0133 \times 10^5\,\mathrm{Pa}$. The time profiles of some reactants and products as well as temperature are displayed in Fig. 1. The oxidation of *n*-heptane takes place in several steps. In a first phase *n*-heptane is decomposed into smaller hydrocarbons. After $5.0 \times 10^{-5}\,\mathrm{s}$ this
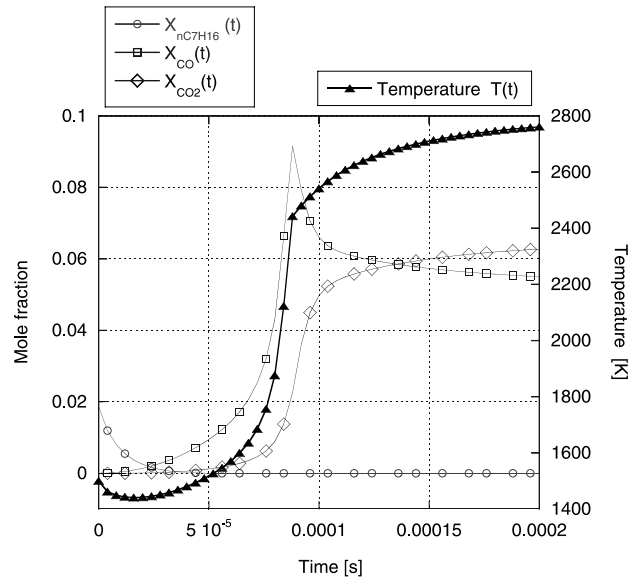
Fig. 1. Time evolution of the species' mole fractions and temperature.

process is completed. At about 8.6×10^{-5} s ignition takes place and CO is converted to CO_2. During this ignition process the number of reactions increases rapidly due to a chain-branching reaction mechanism.

3.2. Approximation

First we study convergence properties of the algorithm. We consider the test example for $t \in [0, 0.0002]s$ so that the ignition point is roughly in the middle of the time interval. The first order approximations (2.32) and (2.33) are used to perform the temperature steps during a single reaction.

The average curves for the temperature are displayed in Fig. 2 for $n = 10^3, 10^4, 10^5, 10^6$ and $nL = 10^7$, where L is the number of independent runs of the particle ensemble used to construct confidence bands. These curves are compared with the results from the code DASSL [1] for solving systems of differential/ algebraic equations. DASSL has been applied successfully to combustion problems as part of the software package SENKIN [15]. We mention that the DASSL-results are contained in the confidence band of the averaged curve for $n = 10^5$ and $n = 10^6$.

The behaviour of both the systematic and the statistical error is highly non-uniform in time. These quantities are displayed in Figs. 3 and 4 for different numbers of particles. Since the product nL is fixed, the curves in Fig. 4 should converge with increasing n, as they indeed do outside a small neighborhood of the ignition point. In that point the fluctuation is so strong that convergence has not yet been reached for the values of n considered. The systematic error increases drastically during and after the ignition time. The statistical error is much larger during the ignition period.

Results for the concentrations of some important species are displayed in Fig. 5. They show that different numbers of particles are needed to resolve the time evolution correctly.

Finally we mention that, applying the iteration scheme (2.35) conserving enthalpy, we observed fast convergence, but did not see any real improvement in the systematic error. Thus the first order approximations (2.32) and (2.33) turn out to be robust enough so that there is only weak accumulation of enthalpy error and no significant influence on temperature.
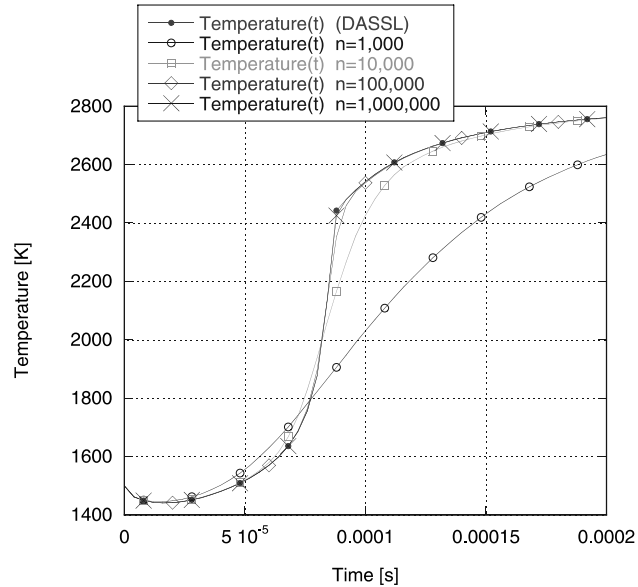
Fig. 2. Time evolution of temperature for different particle numbers. The product of particle number and repetition is constant at $n \times L = 1.0 \times 10^7$.
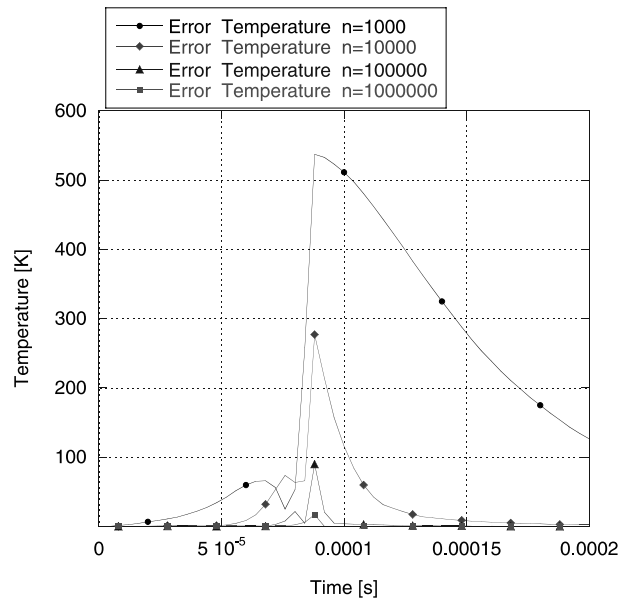

Fig. 3. Error in temperature as a function of time, for different particle numbers.

3.3. Efficiency

Here we discuss the issue of performance for the stochastic algorithm. We compare it, on the one hand, with the deterministic DASSL-algorithm and, on the other hand, with the direct simulation algorithm
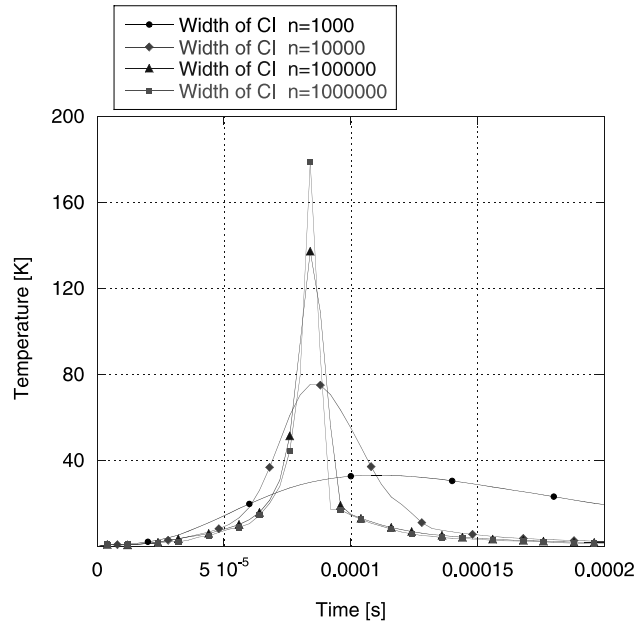
Fig. 4. Width of confidence intervals for temperature as a function of time, for different particle numbers.
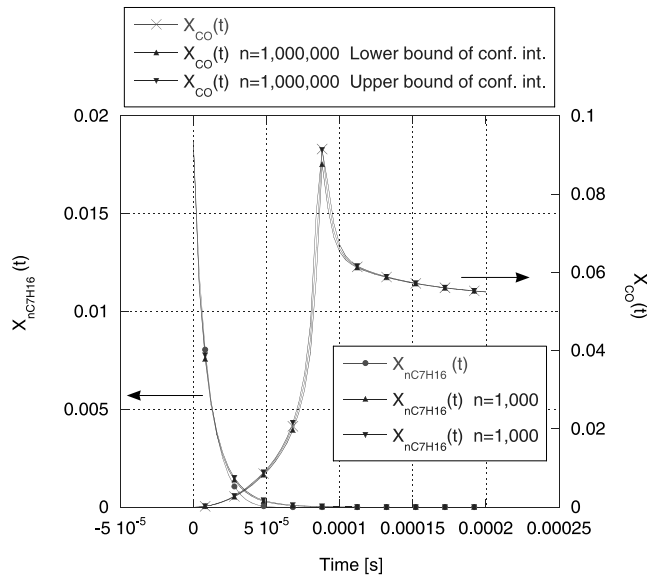
Fig. 5. Heptane and carbon monoxide need different particle numbers to have small errors.

(without combining forward and backward reactions). Note that the computation time required varies with the tolerances used in the error control by DASSL. In our calculations, the default values were used. Increasing these values would reduce the computation time by less than an order of magnitude. However, the general conclusions remain the same.

A basic component influencing the computation time is the *mean number of reactions* $RN(n, t)$. It is easy to see that (cf. (2.51), (2.4), and (2.5))

$$\lim_{n \to \infty} \frac{RN(n, t)}{n} =: a(t) = \int_0^t \lim_{n \to \infty} \frac{1}{n} \pi(Z^{(n)}(s)) \, \mathrm{d}s.$$

The quantity $(\mathrm{d}/\mathrm{d}t)a(t)$ represents the mean number of reactions per particle at time t. It can be expressed via the solution of the problem. Since, according to (2.38), (2.39), (2.44), and (2.21)

$$\lim_{n \to \infty} \frac{1}{n} Q_{\alpha, f}(Z^{(n)}(t)) = \tilde{V}(t) \tilde{M}_\alpha(t) K_{\alpha, f}(T(t)) \prod_{j=1}^{S} [X_j](t)^{v_{\alpha, j}}$$

and

$$\lim_{n \to \infty} \frac{1}{n} Q_{\alpha, r}(Z^{(n)}(t)) = \tilde{V}(t) \tilde{M}_\alpha(t) K_{\alpha, r}(T(t)) \prod_{j=1}^{S} [X_j](t)^{v_{\alpha, j}^*},$$

one obtains

$$\frac{\mathrm{d}}{\mathrm{d}t} a(t) = \tilde{V}(t) \sum_{\alpha=1}^{I} \tilde{M}_\alpha(t) \left| K_{\alpha, f}(T(t)) \prod_{j=1}^{S} [X_j](t)^{v_{\alpha, j}} - K_{\alpha, r}(T(t)) \prod_{j=1}^{S} [X_j](t)^{v_{\alpha, j}^*} \right| \tag{3.1}$$

for the new stochastic algorithm, and

$$\frac{\mathrm{d}}{\mathrm{d}t} a(t) = \tilde{V}(t) \sum_{\alpha=1}^{I} \tilde{M}_\alpha(t) \left[K_{\alpha, f}(T(t)) \prod_{j=1}^{S} [X_j](t)^{v_{\alpha, j}} + K_{\alpha, r}(T(t)) \prod_{j=1}^{S} [X_j](t)^{v_{\alpha, j}^*} \right] \tag{3.2}$$

for the direct simulation algorithm. These formulas clearly show the origin of the efficiency gain of the improved algorithm. Note that the right-hand side in formulas (3.1) and (3.2) can be calculated using the DASSL-solution and used to predict the relative performance of the two stochastic algorithms.
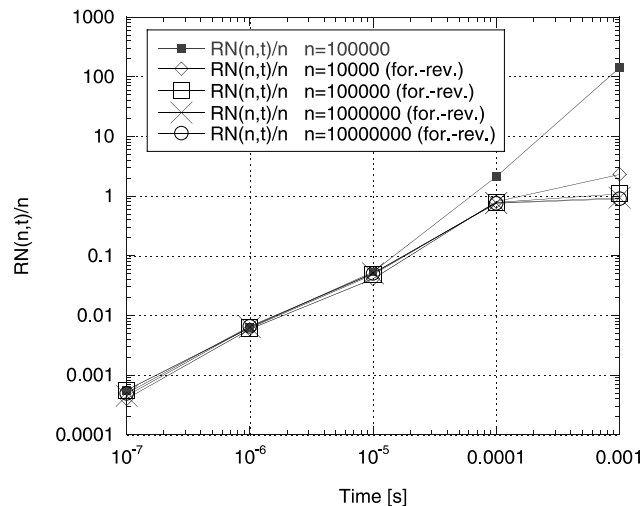

Fig. 6. Normalized reaction numbers for the direct simulation and the improved algorithm.
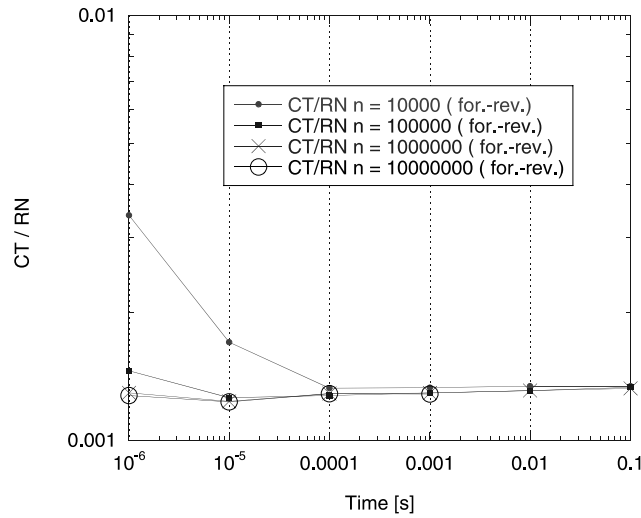
Fig. 7. Computational time divided by reaction number.

A comparison of the normalized reaction numbers for both stochastic algorithms is given in Fig. 6. Up to ignition time their behaviour is very similar. However, during and after ignition the new algorithm leads to a significant decrease of the number of reactions, compared to the original direct simulation algorithm.

Fig. 7 shows the measured *CPU-time* $\mathrm{CT}(n, t)$ for a single run of the algorithm divided by the number of reactions, for varying particle numbers. The observed convergence allows us to conclude that the CPU-time is asymptotically proportional to the number of particles, i.e.
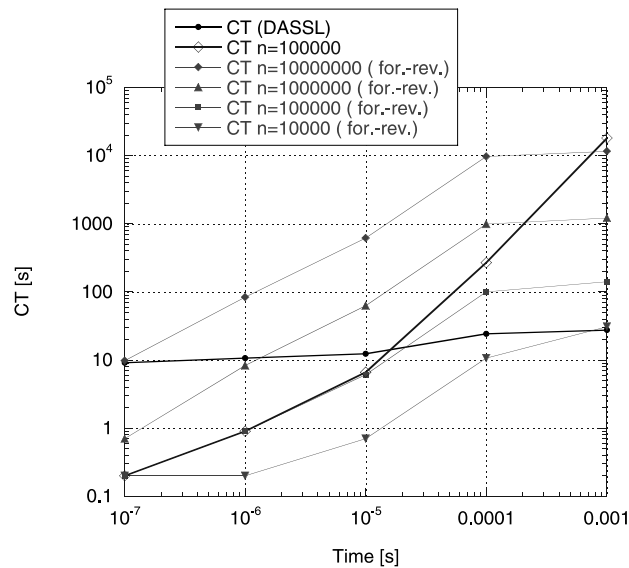

Fig. 8. Computational time as function of simulation time, for different solution methods.

$$\lim_{n\to\infty} \frac{CT(n,t)}{n} =: b(t).$$ (3.3)

Note that the quantity $b(t)/a(t)$ representing the mean effort per reaction does not vary significantly in time.

The absolute values of the CPU-time for a single run of the algorithm are displayed in Fig. 8 for varying particle numbers. It can be seen that the new algorithm outperforms the direct simulation algorithm by a factor 25 up to time $t = 0.0002\,\text{s}$ and by a factor 100 up to time $t = 0.001\,\text{s}$. Fig. 8 shows how the length of the time interval, on which the stochastic algorithm is faster than the deterministic one, depends on the number of particles. The necessary number of particles is determined by the accuracy and depends on the functional to be resolved. For short simulation time the stochastic algorithm is significantly faster than the deterministic algorithm. Using Fig. 8 we conclude that for $n = 10^4$ the stochastic algorithm is faster for simulation times up to 10^{-3}, while for $n = 10^5$ it is faster only for simulation times up to 10^{-5}, and for $n = 10^6$ up to 10^{-6}. These general conclusions can be applied to the quantities displayed in Fig. 5.

4. Concluding remarks

We proposed an improved stochastic algorithm for temperature-dependent homogeneous gas phase reactions. By combining forward and reverse reaction rates, a significant gain in computational efficiency was achieved. Two modifications of modelling the temperature dependence (with and without conservation of enthalpy) were introduced and studied quantitatively. The algorithm was tested for the practically relevant combustion of *n*-heptane.

The numerical studies reveal that

- the algorithm converges to the solution of the deterministic equation;
- combining forward and reverse reactions leads to a significant improvement over the direct simulation method (up to a factor 100, dependent on the time interval);
- the first order temperature scheme is sufficient for practical applications.

In the original formulation of the stochastic algorithm, the presence of forward and backward reactions was basically ignored. Now we combine those pairs to a single type of event, taking into account that the corresponding elementary interactions cancel each other. Formally, the original process can be reproduced by first ignoring reverse reactions by putting their rates equal to zero, and than introducing them as independent reactions.

Finally we mention two main issues for future research. A first direction of study is the further development of the stochastic algorithm. As we have solved the problem of simulating very fast processes by accounting for partial equilibria, the treatment of the slower processes needs further attention. Also the need of high accuracy for several species during ignition should be studied in more detail. A second direction of study is the application of the stochastic algorithm to more complex problems, in which it can successfully compete with its deterministic counterparts. As we have shown, the stochastic algorithm is faster than DASSL, if the time interval is relatively small and the number of particles is not too big. Small time intervals occur in situations where some splitting technique is used to decouple several processes, one of which is chemistry. Moderate particle numbers are of interest in situations where very accurate chemistry calculations are useless, since many other sources of error are involved. A typical such complex problem are chemical processes in a random environment, e.g., in the context of a PDF transport equation approach. Some rather promising first results in this direction are given in [14].

References

[1] K.E. Brenan, S.L. Campbell, L.R. Petzold, Numerical solution of initial-value problems in differential-algebraic equations, Classics in Applied Mathematics, vol. 14, SIAM, 1996.

[2] H.P. Breuer, J. Honerkamp, F. Petruccione, A stochastic approach to complex chemical reations, Chem. Phys. Lett. 190 (3) (1992) 199–201.

[3] H.P. Breuer, W. Huber, F. Petruccione, Fluctuation effects on wave propagation in a reaction-diffusion process, Physica D 73 (1994) 259–273.

[4] D.L. Bunker, B. Garrett, T. Kleindienst, G.S. Long III, Discrete simulation methods in combustion kinetics, Combust. Flame 23 (1974) 373–379.

[5] H.J. Curran, P. Gaffuri, W.J. Pitz, C.K. Westbrook, A comprehensive modeling study of *n*-heptane oxidation, Combust. Flame 114 (1998) 149–177.

[6] D. David, J.-P. Boon, Y.-X. Li, Lattice-gas automata for coupled reaction diffusion equations, Phys. Rev. Lett. 66 (19) (1991) 2535–2538.

[7] S.N. Ethier, T.G. Kurtz, Markov Processes, Characterization and Convergence, Wiley, New York, 1986.

[8] M. Frenklach, Simulation of surface reactions, Pure Appl. Chem. 70 (1998) 477–484.

[9] D.T. Gillespie, A general method for numerically simulating the stochastic time evolution of coupled chemical reactions, J. Comput. Phys. 22 (4) (1976) 403–434.

[10] D.T. Gillespie, Exact stochastic simulation of coupled chemical reactions, J. Phys. Chem. 81 (1977) 2340–2361.

[11] F.A. Houle, W.D. Hinsberg, Stochastic simulations of temperature programmed desorption, Surf. Sci. 338 (1995) 329–346.

[12] R.J. Kee, F.M. Rupley, J.A. Miller, Chemkin-II: A fortran chemical kinetics package for the analysis of gas phase chemical kinetics, Technical Report, Sandia Report SAND89-80009B UC-706, 1989.

[13] M. Kraft, W. Wagner, Numerical study of a stochastic particle method for homogeneous gas phase reactions, Technical Report 570, Weierstraß-Institut für Angewandte Analysis und Stochastik, Berlin, 2000. See http://www.wias-berlin.de/publications/ preprints/570. Comput. Math. Appl. (to appear).

[14] M. Kraft, W. Wagner, An efficient stochastic chemistry approximation for the PDF transport equation, Technical Report 672, Weierstraß-Institut für Angewandte Analysis und Stochastik, Berlin, 2001. See http://www.wias-berlin.de/publications/preprints/ 672.

[15] A.E. Lutz, R.J. Kee, J.A. Miller, SENKIN: A fortran program for predicting homogeneous gas phase chemical kinetics with sensitivity analysis, Technical Report, Sandia Report SAND87-8248 UC-401, 1988.

[16] A.S. McLeod, L.F. Gladden, A Monte Carlo study of temperature-programmed desorption from supported-metal catalysts, Catal. Lett. 55 (1998) 1–6.

[17] H. Wang, Q.-S. Li, Ensemble simulation study of chaos in a chemical model, Phys. Chem. Chem. Phys. 2 (2000) 1951–1953.